



TITLE:

Stimulated emission at 474 nm  
from an InGaN laser diode structure  
grown on a (11 $\bar{2}$ ) GaN  
substrate

AUTHOR(S):

Kojima, K.; Funato, M.; Kawakami, Y.; Masui, S.;  
Nagahama, S.; Mukai, T.

---

CITATION:

Kojima, K. ...[et al]. Stimulated emission at 474 nm from an InGaN laser diode structure grown on a (11 $\bar{2}$ ) GaN substrate. APPLIED PHYSICS LETTERS 2007, 91(25): 251107.

ISSUE DATE:

2007-12-17

URL:

<http://hdl.handle.net/2433/84584>

RIGHT:

Copyright 2007 American Institute of Physics. This article may be downloaded for personal use only. Any other use requires prior permission of the author and the American Institute of Physics.

# Stimulated emission at 474 nm from an InGaN laser diode structure grown on a (11 $\bar{2}2$ ) GaN substrate

K. Kojima,<sup>a),b)</sup> M. Funato,<sup>a)</sup> and Y. Kawakami<sup>a),c)</sup>

*Department of Electronic Science and Engineering, Kyoto University, Kyoto 615-8510, Japan*

S. Masui, S. Nagahama, and T. Mukai

*Nitride Semiconductor Research Laboratory, Nichia Corporation, 491 Oka, Kaminaka, Anan, Tokushima 774-8601, Japan*

(Received 14 September 2007; accepted 26 September 2007; published online 18 December 2007)

The stimulated emissions from semipolar InGaN laser diode (LD) structures grown on (11 $\bar{2}2$ ) GaN substrates are observed at room temperature under photopumped conditions. The measured emission peaks are in the photon energy range from 2.62 eV (474 nm) to 3.05 eV (405 nm), and the emission intensity has a threshold behavior with respect to the pumping power. A strong in-plane optical anisotropy is observed between the two perpendicular directions, [1 1 $\bar{2}3$ ] and [1 $\bar{1}00$ ], due to anisotropic matrix elements, which depend on the crystal orientation; the stimulated emission measured along the [1 1 $\bar{2}3$ ] direction occurs with a lower threshold pumping power at a lower energy compared to that obtained along the [1 $\bar{1}00$ ] direction. The experimental results and the valence band calculations indicate that the transverse-electric mode with an electric vector along the [1 $\bar{1}00$ ] direction is dominant for gain formation in semipolar and nonpolar InGaN LDs. Compared to *c*-plane InGaN LDs, semipolar InGaN LDs have comparable or less threshold pumping powers. © 2007 American Institute of Physics. [DOI: 10.1063/1.2799876]

Current violet and blue InGaN laser diodes (LDs) have low threshold current values and quite high output powers,<sup>1,2</sup> and thus, they can be applied to data storage and laser scanning display devices. However, the longest wavelength of InGaN LDs is limited to 482 nm (Ref. 1) and blue-green and pure green InGaN LDs, which are suitable replacements for solid state or gas lasers and create small coherent light sources, are currently unavailable. We have reported that InGaN LDs that work around 470 nm are affected by quantum confined Stark effect, and believe that crystal growth on non-*c*-plane GaN is one solution to realize blue-green and pure green LDs.<sup>3</sup> Recently, InGaN on non-*c*-plane GaN has received increased attention because of the absence of quantum confined Stark effect, and some groups have already reported LD actions around 400 nm on a nonpolar plane<sup>4,5</sup> and on a semipolar plane.<sup>6</sup> On the other hand, our group has demonstrated efficient luminescence covering blue, green, and even amber colors from semipolar InGaN quantum wells (QWs) grown on the patterned GaN templates and (11 $\bar{2}2$ ) GaN substrates.<sup>7,8</sup> In this article, stimulated emissions over a wide wavelength range, from 474 to 405 nm, are demonstrated for semipolar InGaN LD structures. Furthermore, the unique anisotropic gain formation properties are described and compared to theoretical results.

Three samples with different In contents for the InGaN active layers were grown on the (11 $\bar{2}2$ ) GaN substrates using metal-organic chemical vapor deposition. The samples were labeled as s1, s2, and s3, which have In contents estimated from the optical transition energies of 0.32, 0.29, and 0.17, respectively. The active layers were double QWs and the well widths were set to 2 nm. The QWs were separated by

15-nm-thick GaN barrier layers. The samples had conventional laser structures with doped GaN guiding and AlGaIn cladding layers. Both *n*- and *p*-GaIn were 250 nm thick, but *n*- and *p*-AlGaIn were 1500 and 1000 nm, respectively. The stimulated emission was measured under photopumped conditions at room temperature. The excitation source was an optical parametric oscillator pumped by a Nd: YAG (yttrium aluminum garnet) laser with a pulse width of about 2 ns. The excitation wavelength was 375 nm and active wells were selectively excited. The excited region had a rectangle shape focused by a cylindrical lens, and luminescence was detected from the edge of the sample along the longer side of the excited rectangle region. The samples did not have a cavity structure. Thus, the obtained luminescence was a spontaneous emission amplified by the stimulated emission process with a one pass geometry. We assumed a simple relation for the luminescence intensity *I*, excitation length *L*, and gain *g*,  $I \propto \{\exp(gL) - 1\}/g$ , where *I* increases linearly when *gL* < 1, and increases exponentially when *gL* ≥ 1. Luminescence from the sample was collected into a 25 cm monochromator and detected by a charge coupled device camera. To analyze the anisotropic optical properties of semipolar InGaN QWs, a numerical calculation based on a 6 × 6 wurtzite Hamiltonian<sup>9</sup> in a semipolar QW was performed. A more detailed discussion of the anisotropic properties of semipolar InGaIn will soon appear elsewhere.

Figures 1(a) and 1(b) show the stimulated emission spectra and luminescence intensity, *I<sub>x</sub>*, and *I<sub>y</sub>*, respectively, of s1 as a function of excitation power density taken from different directions. Figure 1(c) details the experimental scheme. To obtain *I<sub>x</sub>*, and *I<sub>y</sub>*, the long side of the excitation rectangle and the detecting direction align along the [1 $\bar{1}00$ ] and [1 1 $\bar{2}3$ ] directions, respectively. The light with an electric vector parallel or perpendicular to (11 $\bar{2}2$ ) is called the TE or TM mode, respectively. Therefore, for example, the electric vector for the TE mode of *I<sub>x</sub>* is parallel to the [1 1 $\bar{2}3$ ] direc-

<sup>a)</sup> Author to whom correspondence should be addressed. Tel: 075-383-2311. Fax: 075-383-2312.

<sup>b)</sup> Electronic mail: kazunobu.kojima@optomater.kuee.kyoto-u.ac.jp

<sup>c)</sup> Electronic mail: kawakami@kuee.kyoto-u.ac.jp

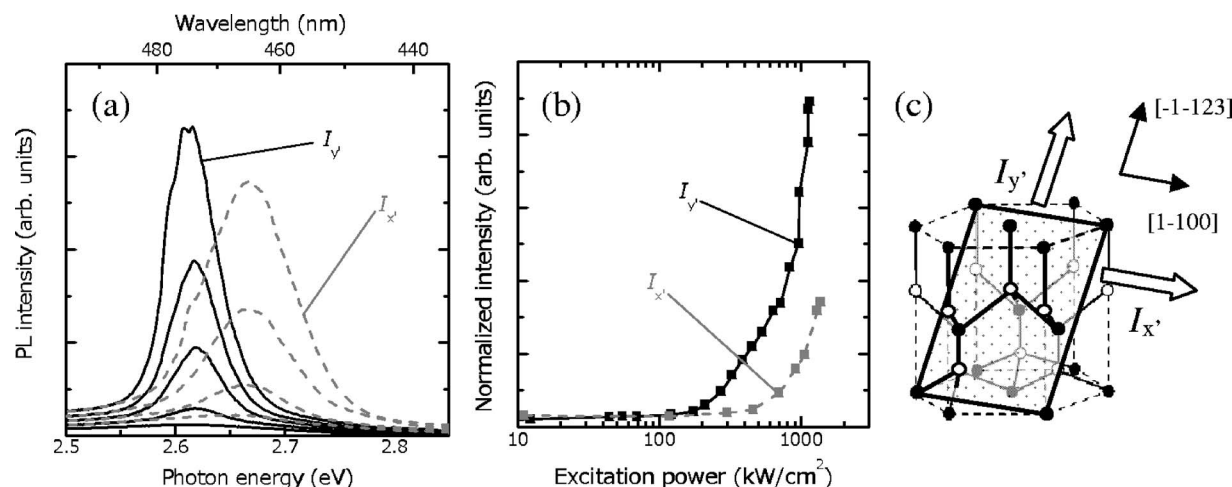


FIG. 1. (a) Stimulated emission spectra of semipolar  $\text{In}_{0.32}\text{Ga}_{0.68}\text{N}$  QWs (sample s1) obtained from two different directions,  $I_x$  and  $I_y$ . (b) Excitation power density vs luminescence intensity. Photoluminescence intensity is normalized by the intensity below the threshold excitation power, which corresponds to a spontaneous process. (c) Measurement scheme to obtain stimulated emission. Light propagating parallel to the  $[1\bar{1}00]$  direction is called  $I'_x$ , while that along  $[1\bar{1}23]$  is labeled as  $I'_y$ .

tion, while that of  $I_y$  is parallel to the  $[1\bar{1}00]$  direction. It is experimentally found that TM-mode luminescence is always quite weak and that the TE-mode light is dominant for both  $I_x$  and  $I_y$ . Hence, we will discuss only the TE-mode luminescence. The estimated threshold power density of  $I_y$  was about  $200 \text{ kW/cm}^2$ , which is much smaller than that of  $I_x$ , which is around  $500 \text{ kW/cm}^2$ , as shown in Fig. 1(b). Furthermore, the peak energy of the stimulated emission for  $I_y$  is a few tens of meV lower than that for  $I_x$ . These tendencies are also observed for the other samples, s2 and s3. To understand the experimental findings, especially the significant differences in the threshold and peak energy, optical matrix elements and optical transition energies were calculated for semipolar InGaN QWs. In the calculation, the valence band Hamiltonian for the wurtzite crystal given in Ref. 9 was diagonalized in the QW structures in order to obtain the valence band structure, and we determined matrix elements of the optical transitions between the conduction band and each valence band.

Figure 2(a) indicates the energy dispersions of a strained bulk  $\text{In}_{0.32}\text{Ga}_{0.68}\text{N}$  coherently grown on the  $(11\bar{2}2)$  GaN substrate without quantum confinement effects. The In content corresponds to that in s1. Typically, semipolar InGaN has three different types of valence bands, which means that there are three different types of holes. The top valence band, named band A, mainly contains characteristics of heavy and

light holes in the  $c$  plane. On the other hand, the second band, called band B, is dominated by characteristics of the crystal-field splitting hole in the  $c$  plane, and thus, the polarizations of the optical transition between electrons and hole A should significantly differ from that of hole B. Figure 2(b) shows the computed crystal orientation dependence of the in-plane polarization of an  $\text{In}_{0.32}\text{Ga}_{0.68}\text{N}/\text{GaN}$  QW with strain (solid lines) and without strain (broken lines). The sign of polarization is defined as follows.<sup>10</sup> When light propagating to the surface normal is dominated by ordinary polarization, the sign of polarization is positive, but when extraordinary light is dominant, the polarization is negative. In the present case, the electric vector of the ordinary light is parallel to the  $[1\bar{1}00]$  direction ( $\perp [0001]$ ), and that of the extraordinary light is parallel to the  $[1\bar{1}23]$  direction, which is vertical to the ordinary one. Thus, it is clear that the electric vectors for the ordinary light and TE mode of  $I_y$  are identical and are related to band A, but those for the extraordinary light and TE mode of  $I_x$  are identical and are related to band B.

According to our theoretical calculations, strained InGaN QWs with a crystal angle more than about  $50^\circ$ , which includes  $(11\bar{2}2)$  QWs, have quite similar optical polarization properties, and the optical transition between an electron and hole A or B are polarized almost linearly, but with the opposite sign. The lowest energy optical transition is between an

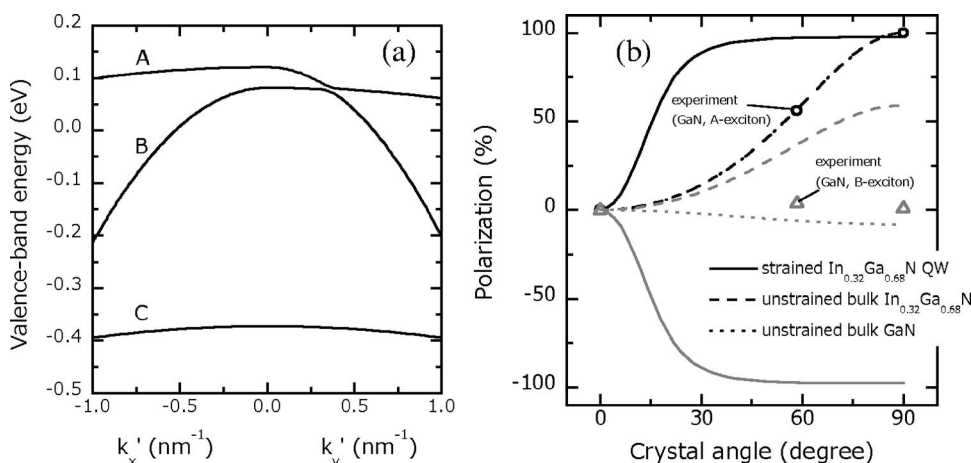


FIG. 2. (a) Energy dispersion of a bulk  $\text{In}_{0.32}\text{Ga}_{0.68}\text{N}$  coherently grown on GaN. (b) Crystal orientation dependence of the polarization of a strained  $\text{In}_{0.32}\text{Ga}_{0.68}\text{N}$  QW on GaN (solid line) as well as unstrained bulk  $\text{In}_{0.32}\text{Ga}_{0.68}\text{N}$  (broken line) and GaN (dotted line). Circles and triangles indicate the measured polarizations of A and B excitons of the unstrained bulk GaN, respectively. In all the cases, black lines correspond to optical transitions between an electron and hole A, while gray lines represent transitions between an electron and hole B.

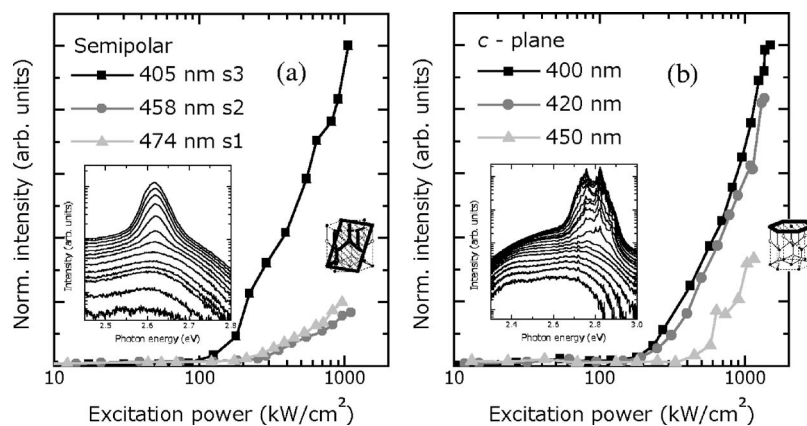


FIG. 3. Threshold behavior of (a) semipolar and (b) *c*-plane InGaN LD structures with different In contents. In the inset of both (a) and (b), luminescence spectra of the samples with longest emitting wavelength are plotted, and excitation power densities range from 5.0 to 525 kW/cm<sup>2</sup> for semipolar LDs and from 13.0 to 1380 kW/cm<sup>2</sup> for *c*-plane LDs. Luminescence intensity is normalized by the intensity under the threshold excitation power corresponding to a spontaneous process.

electron and hole A with the electric vector along the  $[1\bar{1}00]$  direction and has nonzero matrix elements as the TE mode of  $I_y$ , for InGaN QWs grown on the (1122) substrates. On the other hand, the optical transition between an electron and hole B has a matrix element for only the TE mode of  $I_x$ , along the  $[\bar{1}123]$  direction. Moreover, the TM transition, which has an electric vector perpendicular to (1122), always has a zero or negligible component within our calculation. These features quite reasonably explain the experimental results; InGaN QWs grown on the (1122) GaN substrates have only a TE mode gain along the  $[\bar{1}123]$  direction for the lowest transition energy and the second lowest transition has a 90° rotated polarization compared to the lowest one. These correspond to  $I_y$ , and  $I_x$ , respectively. Although the quantum confinement effect and many material parameters should be carefully considered for valence-band calculations, strain due to the lattice mismatch between the active layers and substrate through deformation potentials is the most important physics.

Experimental and theoretical results are also plotted for an unstrained GaN substrate in Fig. 2(b) by symbols and dotted lines, respectively. Although unstrained bulk GaN and In<sub>0.32</sub>Ga<sub>0.68</sub>N have nearly the same tendency for polarization of the optical transition between an electron and hole A, the transition between an electron and hole B has different features due to the difference in the spin-orbit splitting energies. On the other hand, the polarization of a strained In<sub>0.32</sub>Ga<sub>0.68</sub>N QW is far from that of unstrained bulk In<sub>0.32</sub>Ga<sub>0.68</sub>N for both bands. This contrast comes mainly not from quantum confinement effect, but from deformation potentials. We also performed the calculation for strained bulk In<sub>0.32</sub>Ga<sub>0.68</sub>N and found nearly identical results for the case of a strained QW, which suggest a minor effect of confinement on the optical anisotropy. An in-depth discussion will appear elsewhere soon.<sup>11</sup> It is also noteworthy that the differences among (1122) and nonpolar InGaN QWs are negligible in terms of polarization.

Finally, semipolar InGaN LDs are compared to InGaN LDs grown on *c*-plane sapphire substrates. Figure 3 shows luminescence peak intensities of (a) semipolar and (b) *c*-plane InGaN LD structures as a function of excitation power density where the luminescence spectra of the samples with the highest In content are also drawn in the insets. For this measurement, the detecting direction is parallel to  $[\bar{1}123]$ , so that luminescence corresponds to  $I_y$ . The infor-

mation of the *c*-plane InGaN LD structures can be found in Ref. 12. For weaker excitation conditions satisfying  $gL < 1$ , only broad spontaneous emissions are obtained for both types of samples. A narrow luminescence line appears when the excitation exceeds the threshold, which corresponds to  $gL \geq 1$ . Generally, the threshold pumping power increases as the In content of the active layers increases. The threshold photopumping power of s3 is estimated to be 175 kW/cm<sup>2</sup>, while those of s1 and s2 are around 200 kW/cm<sup>2</sup>. These values are comparable to or even less than that of *c*-plane InGaN LDs, which implies that our semipolar laser structures have quality sufficient to *c*-plane ones.

Thus, we have demonstrated stimulated emission from semipolar InGaN LD structures at room temperature in the wavelength range from 405 to 474 nm under photopumped conditions. The stimulated emissions have a clear threshold behavior and show anisotropic optical properties. The threshold pumping power of  $I_y$ , is much lower than that of  $I_x$ . Theoretical calculations, which were performed to analyze the experimental results, agree well with the simulated emissions. Finally, comparing the semipolar InGaN LD structures to the *c*-plane ones demonstrates that both types of LDs show equivalent threshold behaviors.

<sup>1</sup>S. Nagahama, Y. Sugimoto, T. Kozaki, and T. Mukai, Proc. SPIE **5738**, 57 (2005).

<sup>2</sup>T. Kozaki, S. Nagahama, and T. Mukai, Proc. SPIE **6485**, 648503 (2007).

<sup>3</sup>K. Kojima, M. Funato, Y. Kawakami, S. Nagahama, T. Mukai, H. Braun, and U. T. Schwarz, Appl. Phys. Lett. **89**, 241127 (2006).

<sup>4</sup>K. Okamoto, H. Ohta, S. F. Chichibu, J. Ichihara, and H. Takasu, Jpn. J. Appl. Phys., Part 2 **46**, L187 (2007).

<sup>5</sup>M. C. Schmidt, K.-C. Kim, R. M. Farrell, D. F. Feezell, D. A. Cohen, M. Saito, K. Fujito, J. S. Speck, S. P. DenBaars, and S. Nakamura, Jpn. J. Appl. Phys., Part 2 **46**, L190 (2007).

<sup>6</sup>A. Tyagi, H. Zhong, R. B. Chung, D. F. Feezell, M. Saito, K. Fujito, J. S. Speck, S. P. DenBaars, and S. Nakamura, Jpn. J. Appl. Phys., Part 2 **46**, L444 (2007).

<sup>7</sup>K. Nishizuka, M. Funato, Y. Kawakami, Sg. Fujita, Y. Narukawa, and T. Mukai, Appl. Phys. Lett. **85**, 3122 (2004).

<sup>8</sup>M. Ueda, K. Kojima, M. Funato, Y. Kawakami, Y. Narukawa, and T. Mukai, Appl. Phys. Lett. **89**, 211907 (2006).

<sup>9</sup>S. H. Park and S. L. Chuang, Phys. Rev. B **59**, 4725 (1999).

<sup>10</sup>K. Kojima, M. Ueda, M. Funato, and Y. Kawakami, Phys. Status Solidi B **244**, 1853 (2007).

<sup>11</sup>K. Kojima, H. Kamon, M. Ueda, M. Funato, and Y. Kawakami, Phys. Rev. B (to be published).

<sup>12</sup>K. Kojima, M. Funato, Y. Kawakami, Y. Narukawa, and T. Mukai, Solid State Commun. **140**, 182 (2006).